Int. J. Environ. Sci. Technol. (2017) 14:1959–1968
DOI 10.1007/s13762-017-1289-z

ORIGINAL PAPER

Metal-organic framework Uio-66 for adsorption of methylene blue dye from aqueous solutions

A. A. Mohammadi[1] · A. Alinejad[2] · B. Kamarehie[3] · S. Javan[1] · A. Ghaderpoury[4] · M. Ahmadpour[5] · M. Ghaderpoori[3]

Received: 16 August 2016 / Revised: 22 December 2016 / Accepted: 21 February 2017 / Published online: 6 May 2017

Abstract Methylene blue color is a cationic dye which is used in textile industry. Health effects of methylene blue dye discharge into the environment is including toxicity, high color, reduced light penetration in water, high stability, and low degradation capability. So, removing it from the environment is extremely important. The aim of this study was to synthesize Uio-66 MOFs used for adsorption of methylene blue from synthetic sample. The synthesized UiO-66 MOFs were characterized by using XRD, FE-SEM, EDAX, and BET analyses. Various parameters were evaluated such as pH, initial MB concentration, reaction time, and adsorbent dose. The findings showed that the sizes of Uio-66 crystals were between 153 and 213 nm. Total pore volume, BET, and Langmuir surface area were found to be 657, 906 $m^2\ g^{-1}$, and 0.446 $m^3\ g^{-1}$, respectively. Zeta potential of Uio-66 was equal to 6. As a result, at higher than zeta potential point, methylene blue adsorption on Uio-66 is favorable. Maximum adsorption has been achieved at the pH = 9. The maximum adsorption capacity of Uio-66 for methylene blue was 91 mg/g. Optimum dose of Uio-66 was 0.4 g L^{-1} for methylene adsorption. The Langmuir I isotherm was a fit model to describe the adsorption isotherm. Pseudo-first-order kinetic model was a fit model to describe the adsorption kinetic of MB on Uio-66. The Uio-66 MOF is a promising adsorbent in the adsorption of methylene blue from aqueous solution.

Graphical Abstract

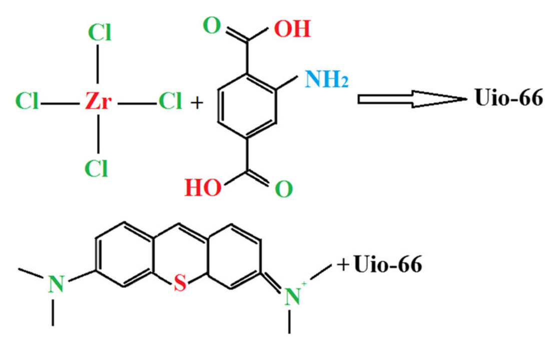

Keywords Dye · Metal-organic frameworks · Porous material · Textile industry

Editorial responsibility: Necip Atar.

✉ M. Ghaderpoori
mghaderpoori@gmail.com

1 Department of Environmental Health Engineering, Neyshabur University of Medical Sciences, Neyshabur, Iran

2 Department of Environmental Health Engineering, Shahid Beheshti University of Medical Sciences, Tehran, Iran

3 Nutrition Health Research Center, Department of Environment Health Engineering, School of Health, Lorestan Medical Sciences University, Khorramabad, Iran

4 Students Research Committee, Department of Environmental Health Engineering, Shahid Beheshti University of Medical Sciences, Tehran, Iran

5 Department of Public Health, Maragheh University of MedicalSciences, Maragheh, Iran

Introduction

Dye is the first thing that is recognized in an effluent. With increasing production of dye and its various applications, there is higher production of effluents with high strength (Rafatullah et al. 2010; Ali et al. 2016; Gupta et al. 2005; Yola et al. 2014a, b). Most materials in effluents are toxic, dangerous and cause severe pollutions in the environment (Rafatullah et al. 2010; Mansoorian et al. 2013; Dias and Petit 2015). One of the most common dyes extensively used in the textile industry is methylene blue which is a cationic dye (Vargas et al. 2011). Till now, various methods for dye adsorption are used, these are, photo-catalytic degradation (Ehrampoosh et al. 2010; Sohrabi and Ghavami 2008), sono-chemical process (Ali et al. 2012), adsorption (Umoren et al. 2013; Ali and Gupta 2006; Ali 2010), H_2O_2 (Masoumbeigi and Rezaee 2015), TiO_2 (Deilami and Fallah 2015), photo-fenton oxidation (Gowtham and Pauline 2015), electro-fenton degradation (Xia et al. 2014) and biological method (Cheng et al. 2015). From these, adsorption is one of the most popular processes. If properly designed, it can effectively remove various dye materials (Crini 2006; Ali 2014). Thus, different adsorbents such as biopolymer oak sawdust composite (El-Latif et al. 2010), mesoporous carbon (Álvarez-Torrellas et al. 2015), waste cotton activated carbon (Ekrami et al. 2016), activated carbon and water hyacinth (Kanawade and Gaikwad 2011), natural illitic clay (Amrhar et al. 2015), modified pumice stone (Derakhshan et al. 2013), zeolite material (Fungaro et al. 2010; Ali et al. 2012), can papyrus (Saed et al. 2014), carbon nanotubes (Shahryari et al. 2010), boron enrichment waste (BW) and molasses modified boron enrichment waste (MBW)-based nanoclays (Gupta et al. 2014), blast furnace sludge (Malina and Radenovic 2014), NaOH-modified dead leaves (Gong et al. 2013), Fe@Au bimetallic nanoparticles (Gupta et al. 2014), TiO_2 nanoparticles involved boron enrichment waste (Yola et al. 2014a, b), wool fiber and cotton fiber (Khan et al. 2005), and bentonite (Hong et al. 2009) are used for adsorption of methylene blue from water and wastewater. These adsorbents have different advantages and disadvantages. With significant development of science in the past decades, considerable progress has been made in the construction and synthesis of new adsorbents (mesoporous materials) (Ali 2012). Metal-organic framework (MOF) is one of these new adsorbents (Hasan et al. 2013; DeCoste and Peterson 2014). Actually, MOFs are a class of porous materials that are composed of two parts: inorganic (as metal core) and organic ligand (as linker) (Katz et al. 2013; Hasan and Jhung 2015). The advantages of these new adsorbents include: high specific surface area, adjustable size by temperature changes, large pore volume and coordinately saturated or unsaturated site to regulate the adsorption capability (Bakhtiari and Azizian 2015; Huo and Yan 2012). MOFs are used in various applications such as advance oxidation processes: (MIL-53, MIL-100(Fe) and FeII@MIL-100(Fe) (Du et al. 2011; Huanli et al. 2015), fluoride (Uio-66) (Massoudinejad et al. 2016), gas separation (Zr-MOF) (Abid et al. 2013; Barea et al. 2014), 2,4-dichlorophenoxyacetic (Jung et al. 2013), phthalic acid and diethyl phthalate (ZIF-8) (Khan et al. 2015), *p*-nitrophenol (HKUST-1) (Lin et al. 2014), arsenate (ZIF-8, MIL-53 and F-BTC) (Li et al. 2014; Zhu et al. 2012). However, the application of Uio-66 in the methylene blue dye adsorption from water and wastewater has not been evaluated. Until now, several metal-organic frameworks are used for adsorption of various dyes such as MOF (Co/Ni) (Abbasi et al. 2016), MIL-125(Ti) (Guo et al. 2015), magnetic $CU_3(BTC)_2$ (Zhao et al. 2015; Lin et al. 2014), Fe(BTC) (García et al. 2014), iron terephthalate (MOF-235) (Haque et al. 2011) and MIL-100(Fe) Huo and Yan 2012). Therefore, the aim of this study was to synthesize Uio-66 MOFs and show its uses in the adsorption of methylene blue from synthetic samples.

Materials and methods

Materials

Zirconium chloride (IV) and terephthalic acid (TPA) were obtained from Merk Company. *N*,*N*-dimethylformamide (DMF), methanol (CH_3OH), methylene blue ($C_{16}H_{18}ClN_3S$), sodium hydroxide (NaOH) and sulfuric acid (H_2SO_4) were supplied by Sigma-Aldrich. All the reagents and solvents were used as received from commercial suppliers without further purification.

Synthesis and preparation of Uio-66

UiO-66 MOF was synthesized according to previous studies (Shen et al. 2013a, b; Luu et al. 2015; Gao et al. 2016). In usual synthesis, 0.2332 g of $ZrCl_4$ [$Zr_6O_4(OH)_4(BDC)_6$] (Furukawa et al. 2013) and 0.161 g terephthalic acid were dissolved in 50 ml DMF solution. Then, the solution was transferred to a 100-ml Teflon autoclave. The autoclave was sealed and heated in a vacuum oven at 120 °C for 48 h under constant pressure. After cooling, the sample was purified with methanol solution (95%) three times to make sure that the occluded DMF molecules were eliminated. After drying, Uio-66 was obtained under vacuum at 100 °C for 12 h.

General characteristics

The synthesized UiO-66 MOF was characterized by X-ray diffraction, field emission-scanning electron microscopy, energy-dispersive X-ray spectroscopy and Brunauer–Emmett–Teller surface area. Total pore volume of the samples was determined by nitrogen (N_2) adsorption isotherms at 77 K.

Adsorption studies

All the experiments of methylene blue adsorption were performed by Uio-66 in batch conditions. The effect of various parameters including pH, initial methylene blue concentration, reaction time, and adsorbent dose was evaluated. Initially, stock solution of methylene blue (1000 mg L^{-1}) was prepared by dissolving 1 g of methylene blue in 1 L of distilled water and then stored under standard conditions. An adsorbent dose was added to 50 ml of methylene blue solution. The solution pH was adjusted by using 0.1 N NaOH and HCl. After the experiments, the remaining adsorbent was separated from the solution by centrifugation (2000 rpm and 15 min). Then, the residual methylene blue concentration was determined by a spectrophotometer ($\lambda = 624$ nm) (Li et al. 2014). All the experiments were done at constant temperature of 25 ± 1 °C (Cai et al. 2015). Finally, the amount of methylene blue adsorbed on the Uio-66 was calculated according to Eq. 1 (Reardon and Wang 2000):

$$q_e = \frac{V(C_0 - C_e)}{m} \quad (1)$$

where C_0 and C_e are the concentration of initial and final methylene blue in the solution (mg L^{-1}), respectively, V is the volume of methylene blue solution (ml), and m is the weight of the adsorbent (g). The removal efficiency of methylene blue was calculated according to Eq. 2 (Bhaumik et al. 2013):

$$R\ (\%) = \frac{(C_0 - C_t)}{C_0} \quad (2)$$

where C_0 and C_t represent the initial and final methylene blue concentration (mg L^{-1}), respectively.

Results and discussion

X-ray diffraction analysis

X-ray diffraction (XRD) pattern is a useful tool for identification of the atomic and molecular structures of a crystal sample. The as-synthesized Uio-66 was in the form of white powder. The crystallographic structure of synthesized Uio-66 was investigated by X-ray diffraction. The X-ray diffraction pattern of the prepared Uio-66 is shown in Fig. 1. The Uio-66 MOF contained characteristic peaks at 2θ equal to 7° and 8.45° with variation of peak intensity depending on the reaction time (Luu et al. 2015). X-ray diffraction pattern was similar to that of previous studies (Lin et al. 2016; Peterson et al. 2014; Shen et al. 2013a, b). Also, Fig. 2 shows FTIR spectra of the prepared Uio-66.

Field emission-scanning electron microscopy (FE-SEM)

Figure 2 shows the SEM morphology of as-synthesized Uio-66. The field emission-SEM image showed that the sizes of Uio-66 crystals were between 153 and 213 nm. In similar studies, the prepared Uio-66 MOFs crystals sizes were between 200 and 500 nm (Lin et al. 2015).

The nitrogen adsorption–desorption isotherms

Figure 3 shows N_2 adsorption–desorption isotherms and BJH pore size distributions of Uio-66 MOFs. Adsorption–desorption isotherm of Uio-66 was similar to type I. Table 1 shows some properties of the prepared Uio-66 MOFs.

Energy-dispersive X-ray spectroscopy (EDAX)

Energy-dispersive X-ray spectroscopy is an analytical technique used for the elemental analysis or chemical composition of one sample (Masoumbeigi and Rezaee 2015). In this work, energy-dispersive X-ray spectroscopy technique was utilized to check the chemical composition of the synthesized Uio-66. The results showed that percentages of C, O, Zr, and Cl compounds were 46.84, 23.65, 26.64, and 2.87%, respectively. As shown in the results, the ingredients of as-synthesized Uio-66 were the same with the raw materials used before that without any impurity.

Effect of pH

pH is one of the most important parameters that influence dye adsorption, because of change in the surface charges of adsorbent and the degree of ionization of the target pollutants (Guo et al. 2015; Lin et al. 2014). So, the initial pH of the methylene blue solution is a significant factor. In this work, methylene blue adsorption by Uio-66 MOF was studied in various pH_s and at 298 °K. To evaluate the effect of pH on methylene blue adsorption, various pH_s in the range of 3–11 were used. In the adsorption experiments, a 0.4 g of Uio-66 MOF was added to 50 ml volume of methylene blue solution with initial concentration of 30 mg L^{-1}. Figure 4 shows methylene blue adsorption at various pH_s. Increasing pH from 3 to 11 led to methylene blue adsorption. At pH of 3 and 9, methylene blue adsorption was 10.3 and 80.96%, respectively. Uio-66 with pH = 9 can remove large amount of methylene blue. In Lin study, methylene blue adsorption efficiency increased with increase in pH (Lin et al. 2014). Methylene blue dye is a cationic dye. At low pH, H^+ concentration is high, so, Uio-66 surface charge is positive which in turn reduces the methylene blue adsorption. By increasing pH, OH^-

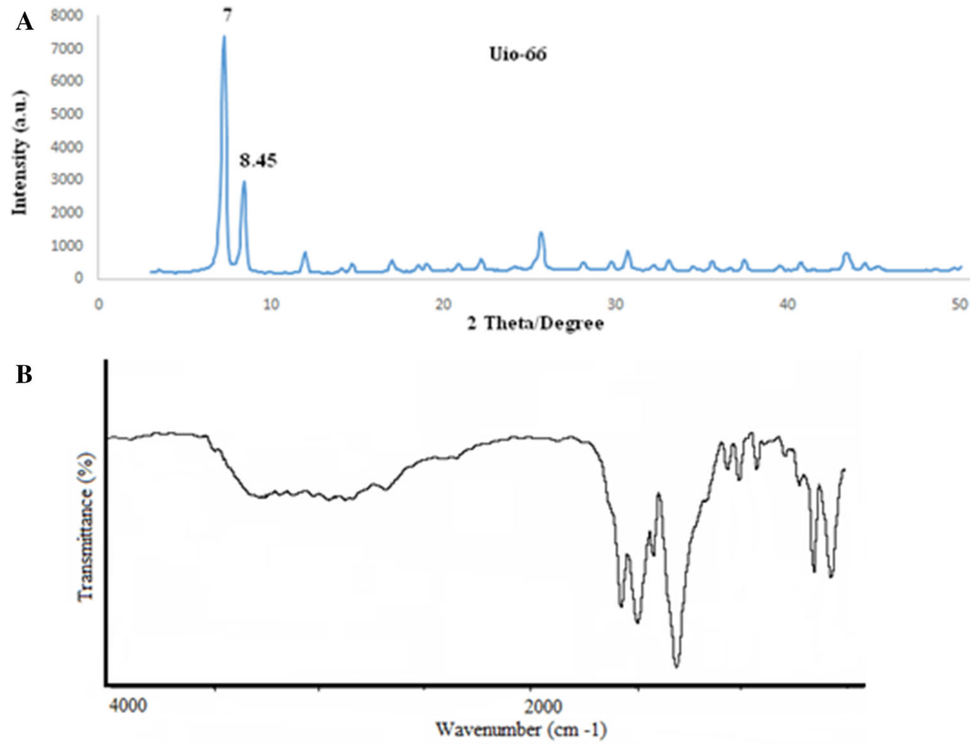

Fig. 1 **a** X-ray diffraction pattern of the prepared Uio-66, **b** FTIR spectra of the prepared Uio-66

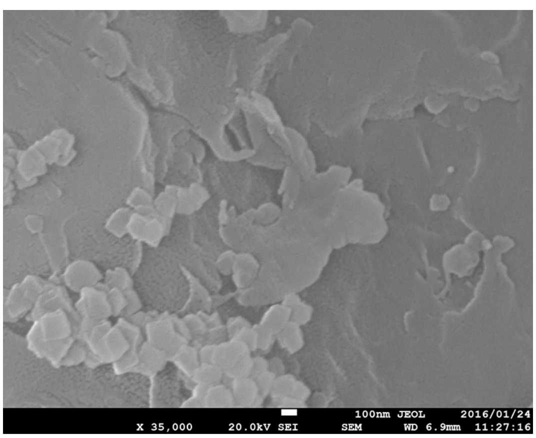

Fig. 2 Field emission-SEM image of the prepared Uio-66 MOFs

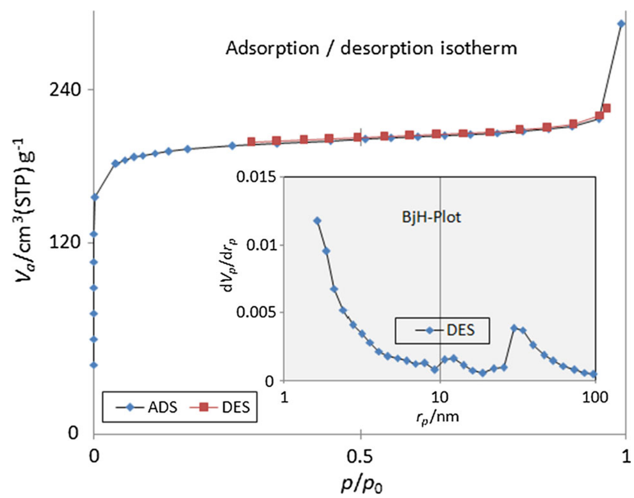

Fig. 3 N_2 adsorption–desorption isotherm and BJH pore size distributions of Uio-66

concentration gradually increased and methylene blue adsorption on Uio-66 increased (Weng and Pan 2007; Gürses et al. 2006). Isoelectric point of Uio-66 was equal to 6. At pH higher than isoelectric point, methylene blue adsorption on Uio-66 was favorable. Maximum adsorption was achieved at pH 9. As a result, pH 9 was selected for further experiment.

Effect of initial concentration of methylene blue dye

In order to evaluate the effect of initial concentration, 10–50 mg L^{-1} methylene blue concentration was used at contact time of 60 min. Figure 5 shows the effect of initial methylene blue concentration on adsorption by Uio-66. With increasing methylene blue concentration, adsorption efficiency decreased. In methylene blue equal to 10 mg L^{-1}, methylene blue dye was completely adsorbed after 300 min contact time. In lower concentrations, methylene blue molecules were adsorbed on Uio-66 adsorbent surface, rapidly, but Uio-66 surface became saturated gradually with increase in methylene blue. Finally, the adsorption decreased because of the repulsion among methylene blue

Table 1 Some properties of Uio-66 for BET experiments at 77 K

Sample	SA_{BET} (m^2 g^{-1})	$SA_{Langmuir}$ (m^2 g^{-1})	Total pore volume (m^3 g^{-1})	Mean pore diameter (nm)
Uio-66	765	906	0.446	2.331

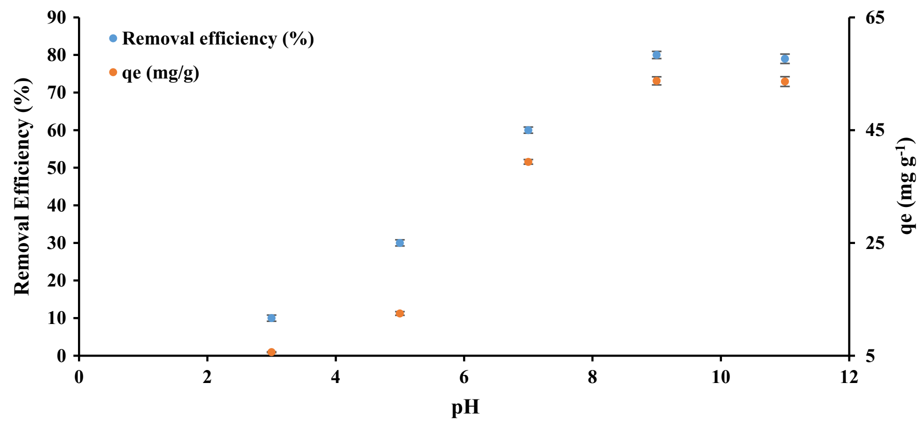

Fig. 4 The effect of pH on methylene blue adsorption by Uio-66 MOF

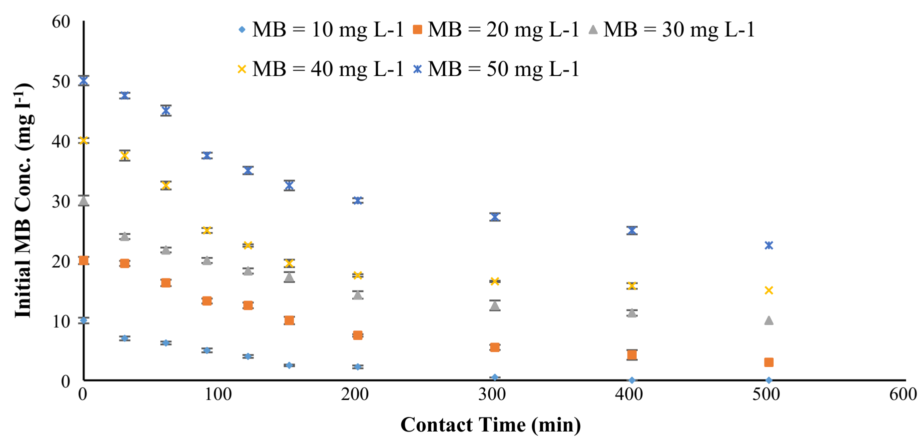

Fig. 5 The effect of initial methylene blue concentration versus contact time

molecules (García et al. 2014; Zvinowanda et al. 2009).

Effect of Uio-66 dose

Figure 6 shows the effect of Uio-66 dose and removal efficiency of methylene blue dye. It was observed that methylene blue adsorption increased with the increase in Uio-66 dose until an equilibrium dose was reached. Optimum dose was 0.4 g L^{-1}. With increase in the Uio-66 dose, methylene blue adsorption was not significant. Adsorption efficiency of methylene blue in dosages of 0.4 and 0.5 g L^{-1} were 72.5 and 75%, respectively. As a result, the optimum dose was 0.4 g L^{-1}. Based on the finding of other researchers, the increase in methylene blue adsorption with Uio-66 dose can be caused by high adsorbent surface and availability of more adsorption sites

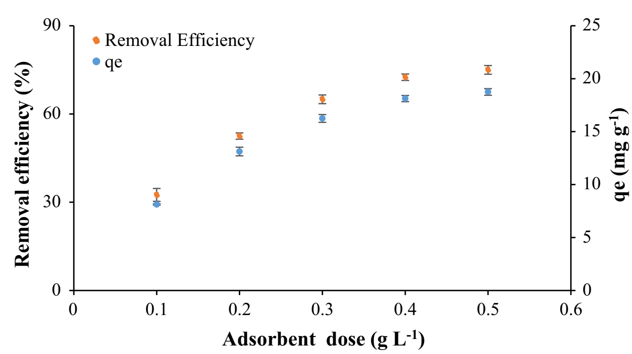

Fig. 6 The effect of adsorbent dose of Uio-66 on methylene blue adsorption

(Maleki et al. 2015). With dose higher than optimum (0.4 g L^{-1}) and with increase in Uio-66 dose, adsorption capacity of adsorbent was almost constant. This

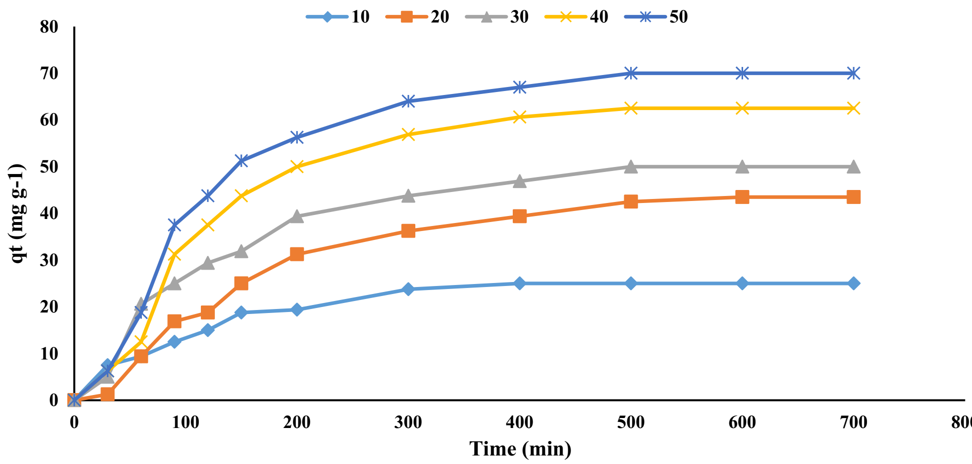

Fig. 7 Effect of initial methylene blue concentration and contact time on Uio-66 MOF

phenomenon can be due to overlapping or aggregation of adsorption sites of Uio-66 that eventually lead to decrease in total Uio-66 surface area (Maleki et al. 2015; Zhang et al. 2014).

Adsorption kinetics and adsorption isotherms

In order to study the mechanisms of methylene blue adsorption on Uio-66, kinetic models like pseudo-first-order and pseudo-second-order kinetic models were used. The pseudo-first-order kinetic model expression of Lagergren is expressed in Eq. 3:

$$\frac{dq_t}{dt} = k_1(q_e - q_t)^2 \quad (3)$$

where q_e and q_t are the amounts of methylene blue adsorbent on the Uio-66 at equilibrium and at time t, respectively, and k_1 is the rate constant (min^{-1}). The linear form of pseudo-first-order is expressed as Eq. 4 (Baskan and Pala 2011; Mohsenibandpei et al. 2016)

$$\log(q_e - q_t) = \log q_e - \frac{k_1}{2.303}t \quad (4)$$

where k_1 and q_e are obtained from the slope and intercept of the linear plots of log $(q_e - q_t)$ versus t, respectively. Pseudo-second-order kinetics model is expressed as Eq. 5 (Kragović et al. 2013; Mohsenibandpei et al. 2016):

$$\frac{dq_t}{dt} = k_2(q_e - q_t)^2 \quad (5)$$

where q_t and q_e are sorbent methylene blue at time t and equilibrium (mg L^{-1}), respectively, and k_2 is the constant of pseudo-second-order sorption of methylene blue (g mg^{-1} min^{-1}). The linear form of pseudo-second-order is expressed in Eq. 6:

$$\frac{t}{q_t} = \frac{1}{k_2 q_e^2} + \frac{t}{q_e} \quad (6)$$

where k_2 and q_e are obtained from the slope and intercept of the linear plots of $\log(q_e - q_t)$ versus t, respectively. To conduct adsorption kinetic experiments, 0.4 g of Uio-66 adsorbent was added to 50 ml of methylene blue solution at initial concentration of 10–50 mg L^{-1}. Figure 7 shows the effect of initial methylene blue concentration and contact time on methylene blue adsorption on Uio-66 MOF. Initially, methylene blue dye was adsorbed rapidly on Uio-66. Adsorption equilibrium of methylene blue was performed after 200 min. After this time, methylene blue adsorption dose did not significantly change. Calculated constants of kinetic models are given in Table 2. Coefficient of determination (R^2) was used to determine the best kinetic model (Bakhtiari and Azizian 2015). Coefficient of determination of the used kinetic models is given in Table 2. As shown in Table 2, pseudo-first-order (PFR) kinetic model had the highest square R. As a result, the PFR model was a fit model to describe the adsorption kinetic of methylene blue on Uio-66.

Adsorption isotherms were used to describe the adsorption of methylene blue and mechanisms of adsorption on Uio-66. The adsorption of methylene blue on Uio-66 MOF was studied with five concentrations (10, 20, 30, 40, and 50 mg L^{-1}), various contact times (30–500 min) at temperature and stirring speed of 298 °K and 300 rpm, respectively. In this research, the equilibrium data of Uio-66 were fitted to the Langmuir (I, II, III, and IV) and Fraundlich isotherms. The Fraundlich isotherm model is expressed in Eq. 7 (Camacho et al. 2011):

$$q_e = K_f C_e^{1/n} \quad (7)$$

where q_e is the amount of methylene blue adsorbed at equilibrium, C_e is the equilibrium concentration of methylene blue in the solution, and K_f and n are the Fraundlich constants. The linear form of the Fraundlich isotherm model is expressed in Eq. 8 (Lee and Tiwari 2013):

Table 2 Calculated constants of kinetic models for the adsorption of methylene blue on Uio-66

Kinetics type	Kinetic parameters	MB concentration (mg L^{-1})				
		10	20	30	40	50
Pseudo-first-order reaction	K_1	0.0171	0.0082	0.0071	0.0071	0.0072
	R^2	0.9944	0.9982	0.9948	0.9905	0.9957
	q_{cal}	53.8368	56.8787	50.2925	55.1593	81.3564
Pseudo-second-order reaction	K_2	0.00040	0.00000	0.00021	0.00008	0.00004
	R^2	0.9539	0.0188	0.9600	0.7417	0.6204
	q_m	29.2830	192.4024	56.1478	84.4895	103.5427

$$\log q_e = \frac{1}{n}\log C_e + \log K_f \tag{8}$$

where q_e and C_e are the amount adsorbent of methylene blue (mg g^{-1}) and sorption concentration (mg L^{-1}) at equilibrium, respectively. K_F and 1/n are the Fraundlich constants denoting adsorption capacity and adsorption intensity or surface heterogeneity, respectively. The Langmuir isotherm model is expressed in Eq. 9 (Jayakumar et al. 2015):

$$q_e = \frac{q_m K_L C_e}{1 + K_L C_e} \tag{9}$$

where q_e and q_m are amount of adsorbed methylene blue per unit mass of Uio-66 and maximum sorption capacity of the Uio-66 (mg g^{-1}), respectively. C_e is equilibrium methylene blue concentration, and K_L is Langmuir isotherm constant (dm^3 g^{-1}). The linear form of the Langmuir isotherm model is expressed as Eq. 10 (Jayakumar et al. 2015):

$$\frac{C_e}{q} = \frac{1}{q_0 b} + \frac{C_e}{q_e} \tag{10}$$

where q is the amount of methylene blue adsorbed per unit weight of Uio-66 (mg g^{-1}) at equilibrium, C_e is the equilibrium methylene blue concentration (mg L^{-1}), q_0 is the Langmuir monolayer adsorption capacity, and b is the Langmuir constant (L g^{-1}). Calculated constants of kinetic models are given in Table 3. Coefficient of determination (R^2) was used to determine the best isotherm model (Huo and Yan 2012). R squared or coefficient of determination is a number that indicates the proportion of the variance in the dependent variable which is predictable from the independent variable (Steel and Torrie 1960). Coefficient of determination of the used isotherm models is shown in Table 3. As illustrated in Table 3, Langmuir I model has the highest R^2 (0.9993). As a result, the Langmuir I isotherm was the best fit model to describe the adsorption isotherm of methylene blue on Uio-66. According to Langmuir I model, the maximum adsorption capacity (q_m) (for initial methylene blue concentration, 10–50 mg L^{-1}) of Uio-66 for methylene blue adsorption was equal to 64.5 mg g^{-1}.

Table 3 Calculated constants of isotherm models for the adsorption of methylene blue onto Uio-66

Isotherm type		Isotherm parameters	Adsorbent dose (g L^{-1})
Fraundlich		n	3.1926
		K_f	23.6945
		R^2	0.9682
Langmuir	I type	K_L	0.5281
		R^2	0.9993
		q_m	90.4840
	II type	K_L	0.6338
		R^2	0.9973
		q_m	70.7695
	III type	K_L	0.6134
		R^2	0.9877
		q_m	65.4031
	IV type	K_L	0.6059
		R^2	0.9877
		q_m	70.6084

Regeneration studies

One of the most important issues in the adsorption processes is reuse of the used adsorbent. In this work, Uio-66 was regenerated with methanol. To do so, 0.4 of Uio-66 was added to 50 ml of methylene blue solution (initial concentration = 20 mg L^{-1}). After completion of methylene blue adsorption process, the used Uio-66 was separated. For the regeneration of the used Uio-66, methanol was applied with high purity of 95%. After washing with methanol, the adsorbent was dried in an oven at 100 °C for 10 h. Regeneration process was performed with 5 cycles. The results showed that Uio-66 MOFs can be easily regenerated with methanol and methylene blue adsorption efficiency which is almost unchanged after multiple times.

Conclusion

In this research, Uio-66 was synthesized using hydrothermal method. It was used for the adsorption of methylene blue dye from synthetic samples. Uio-66 structure was characterized by using X-ray diffraction, Fourier transform infrared spectroscopy spectra, field emission-scanning electron microscopy, energy-dispersive X-ray spectroscopy, and Brunauer–Emmett–Teller. Adsorption isotherm of methylene blue was described based on Langmuir model that represents the monolayer adsorption onto Uio-66. The best kinetic model for methylene blue adsorption is a more suitable pseudo-first-order model. The maximum adsorption capacity of Uio-66 MOFs was 90 mg g^{-1} at an initial concentration of 50 mg L^{-1}. The Uio-66 MOFs is a promising adsorbent in the adsorption of methylene blue from aqueous solution.

Acknowledgements The authors thank Neyshabur University of Medical Sciences for supporting the research (No. 140).

References

Abbasi A, Soleimani M, Najafi M, Geranmayeh S (2016) New interpenetrated mixed (Co/Ni) metal-organic framework for dye removal under mild conditions. Inorg Chim Acta 439:18–23

Abid HR, Shang J, Ang HM, Wang S (2013) Amino-functionalized Zr–MOF nanoparticles for adsorption of CO_2 and CH_4, desalination and water treatment. Int J Smart Nano Mater 4:72–82

Ali I (2010) The quest for active carbon adsorbent substitutes: inexpensive adsorbents for toxic metal ions removal from wastewater. Sep Purif Rev 39:95–171

Ali I (2012) New generation adsorbents for water treatment. Chem Rev 112:5073–5091

Ali I (2014) Water treatment by adsorption columns: evaluation at ground level. Sep Purif Rev 43:175–205

Ali I, Gupta VK (2006) Advances in water treatment by adsorption technology. Nat Protoc 1:2661–2667

Ali I, Mohd A, Khan TA (2012) Low cost adsorbents for removal of organic pollutants from wastewater. J Environ Manag 113:170–183

Ali I, Al-Othman ZA, Alwarthan A (2016) Molecular uptake of congo red dye from water on iron composite nano particles. J Mol Liquid 224:171–176

Álvarez-Torrellas S, García-Lovera R, Rodríguez A, García J (2015) Removal of methylene blue by adsorption on mesoporous carbon from peach stones. Chem Eng Trans 43:2283–9216

Amrhar O, Nassali H, Elyoubi MS (2015) Modeling of adsorption isotherms of methylene blue onto natural illitic clay: nonlinear regression analysis. AMRHAR Moroc J Chem 3:582–593

Bakhtiari N, Azizian S (2015) Adsorption of copper ion from aqueous solution by nanoporous MOF-5: a kinetic and equilibrium study. J Mol Liquid 206:114–118

Barea E, Montoro C, Navarro JA (2014) Toxic gas removal-metal-organic frameworks for the capture and degradation of toxic gases and vapours. Chem Soc Rev 43:5419–5430

Baskan MB, Pala A (2011) Removal of arsenic from drinking water using modified natural zeolite. Desalination 281:396–403

Bhaumik R, Mondal NK, Chattoraj S, Datta JK (2013) Application of response surface methodology for optimization of fluoride removal mechanism by newly developed biomaterial. Am J Anal Chem 4:404–419

Cai HM, Chen GJ, Peng CY, Zhang ZZ, Dong YY, Shang GZ, Zhu XH, Gao HJ, Wan XC (2015) Removal of fluoride from drinking water using tea waste loaded with Al/Fe oxides: a novel, safe and efficient biosorbent. Appl Surf Sci 328:34–44

Camacho LM, Parra RR, Deng S (2011) Arsenic removal from groundwater by MnO_2-modified natural clinoptilolite zeolite: effects of pH and initial feed concentration. J Hazard Mater 189:286–293

Cheng M, Zeng G, Huang D, Lia C, Wei Z, Li N, Xu P, Zhang C, Zhu Y, Hu X (2015) Combined biological removal of methylene blue from aqueous solutions using rice straw and *Phanerochaete chrysosporium*. Appl Microbiol Biotechnol 99:5247–5256

Crini G (2006) Non-conventional low-cost adsorbents for dye removal: a review. Bioresour Technol 97:1061–1085

DeCoste JB, Peterson GW (2014) Metal-organic frameworks for air purification of toxic chemicals. Chem Rev 114:5695–5727

Deilami M, Fallah N (2015) Dye removing from industrial wastewater by advanced oxidation process, biological forum. Int J 7:490–1498

Derakhshan Z, Baghapour MA, Ranjbar M, Faramarzian M (2013) Adsorption of methylene blue dye from aqueous solutions by modified pumice stone: kinetics and equilibrium studies. Health Scope 2:136–144

Dias EM, Petit C (2015) Towards the use of metal-organic frameworks for water reuse: a review of the recent advances in the field of organic pollutants removal and degradation and the next steps in the field. J Mater Chem A 3:22484–22506

Du JJ, Yuan YP, Sun JX, Peng FM, Jiang X, Qiu LG, Xie AJ, Shen YH, Zhu JF (2011) New photocatalysts based on MIL-53 metal-organic frameworks for the decolorization of methylene blue dye. J Hazard Mater 190:945

Ehrampoosh MH, Moussavi SGH, Ghaneian MT, Rahimi S, Fallahzadeh H (2010) A comparison between tubular and batch reactors in removal of methylene blue dye from simulated textile wastewater using TiO_2/UV-C photo catalytic process. Toloo-e-behdasht 1:1–10

Ekrami E, Dadashian F, Arami M (2016) Adsorption of methylene blue by waste cotton activated carbon: equilibrium, kinetics, and thermodynamic studies. Desalination Water Treat 57:7098–7108

El-Latif MA, Ibrahim AM, El-Kady M (2010) Adsorption equilibrium, kinetics and thermodynamics of methylene blue from aqueous solutions using biopolymer oak sawdust composite. J Am Sci 6:267–283

Fungaro DA, Grosche LC, Pinheiro AS, Izidoro JC, Borrely SI (2010) Adsorption of methylene blue from aqueous solution on zeolitic material and the improvement as toxicity removal to living organisms. Orbital 2:235–247

Furukawa H, Cordova KE, O'Keeffe M, Yaghi OM (2013) The chemistry and applications of metal-organic frameworks. Science 341:1230444

Gao S-T, Liu W, Feng C, Shang N-Z, Wang C (2016) A Ag–Pd alloy supported on an amine-functionalized UiO-66 as an efficient synergetic catalyst for the dehydrogenation of formic acid at room temperature. Catal Sci Technol 6:869–874

García ER, Medina RL, Lozano MM, Pérez IH, Valero MJ, Franco AMM (2014) Adsorption of azo-dye orange ii from aqueous

solutions using a metal-organic framework material: iron-benzenetricarboxylate. Materials 7:8037–8057
Gong L, Sun W, Kong L (2013) Adsorption of methylene blue by NaOH-modified dead leaves of plane trees. Comput Water Energy Environ Eng 2:13–19
Gowtham B, Pauline S (2015) feasibility studies on application of photo-Fenton oxidation for methylene blue. Iran J Energy Environ 6:255–259
Guo H, Lin F, Chen J, Li F, Weng W (2015) Metal-organic framework MIL-125(Ti) for efficient adsorptive removal of Rhodamine B from aqueous solution. Appl Organomet Chem 29:12–19
Gupta VK, Ali I, Saini VK, Van Gerven T, Van der Bruggen B, Vandecasteele C (2005) Removal of dyes from wastewater using bottom ash. Ind Eng Chem Res 44:3655–3664
Gupta VK, Atar N, Yola ML, Üstündağ Z, Uzun L (2014) A novel magnetic Fe@ Au core–shell nanoparticles anchored graphene oxide recyclable nanocatalyst for the reduction of nitrophenol compounds. Water Res 48:210–217
Gürses A, Doğar C, Yalc M, Acıkyıldız M, Karaca S (2006) The adsorption kinetics of the cationic dye, methylene blue, onto clay. J Hazard Mater B131:217–228
Haque E, Jun JW, Jhung SH (2011) Adsorptive removal of methyl orange and methylene blue from aqueous solution with a metal-organic framework material, iron terephthalate (MOF-235). J Hazard Mater 185:507–511
Hasan Z, Jhung SH (2015) Removal of hazardous organics from water using metal-organic frameworks (MOFs): plausible mechanisms for selective adsorptions. J Hazard Mater 283:329–339
Hasan Z, Choi EJ, Jhung SH (2013) Adsorption of naproxen and clofibric acid over a metal-organic framework MIL-101 functionalized with acidic and basic groups. Chem Eng J 219:537–544
Hong S, Cheng W, He J, Gan F, Ho YS (2009) Adsorption thermodynamics of methylene blue onto bentonite. J Hazard Mater 167:630–633
Huanli L, Zhao H, Cao T, Qian L, Wang Y, Zhao G (2015) Efficient degradation of high concentration azo-dye wastewater by heterogeneous Fenton process with iron-based metal-organic framework. J Mol Catal A Chem 400:81–89
Huo SH, Yan XP (2012) Metal-organic framework MIL-100(Fe) for the adsorption of malachite green from aqueous solution. J Mater Chem 22:7449–7455
Jayakumar R, Rajasimman M, Karthikeyan C (2015) Optimization, equilibrium, kinetic, thermodynamic and desorption studies on the sorption of Cu(II) from an aqueous solution using marine greenalgae: *halimeda gracilis*. Ecotoxicol Environ Saf 121:199–210
Jung BK, Hasan Z, Jhung SH (2013) Adsorptive removal of 2,4-dichlorophenoxyacetic acid (2,4-D) from water with a metal-organic framework. Chem Eng J 234:99–105
Kanawade SM, Gaikwad RW (2011) Removal of methylene blue from effluent by using activated carbon and water hyacinth as adsorbent. Int J Chem Eng Appl 2:317–319
Katz MJ, Brown ZJ, Colon YJ, Siu PW, Scheidt KA, Snurr RQ, Hupp JT, Farha OK (2013) A facile synthesis of UiO-66, UiO-67 and their derivatives. Chem Commun 49:9449–9451
Khan AR, Tahir H, Uddin F, Hameed U (2005) Adsorption of methylene blue from aqueous solution on the surface of wool fiber and cotton fiber. J Appl Sci Environ Manag 9:29–35
Khan NA, Jung K, Hasan Z, Jhung SH (2015) Adsorption and removal of phthalic acid and diethyl phthalate from water with zeolitic imidazolate and metal-organic frameworks. J Hazard Mater 282:194–200
Kragović M, Daković A, Marković M, Krstić J, Gatta GD, Rotiroti N (2013) Characterization of lead sorption by the natural and Fe(III)-modified zeolite. Appl Surf Sci 283:764–774
Lee SM, Tiwari D (2013) Manganese oxide immobilized activated carbons in the remediation of aqueous wastes contaminated with copper(II) and lead(II). Chem Eng J 225:128–137
Li J, Wu YN, Li Z, Zhang B, Zhu M, Hu X, Zhang Y, Li F (2014) Zeolitic imidazolate framework-8 with high efficiency in trace arsenate adsorption and removal from water. J Phys Chem 118:27382–27387
Lin S, Song Z, Che G, Ren A, Li P, Liu C, Zhang J (2014) Adsorption behavior of metal-organic frameworks for methylene blue from aqueous solution. Microporous Mesoporous Mater 193:27–34
Lin KYA, Chen SY, Jochems AP (2015) Zirconium-based metal organic frameworks: highly selective adsorbents for removal of phosphate from water and urine. Mater Chem Phys 160:168–176
Lin KYA, Liu YT, Chen SY (2016) Adsorption of fluoride to UiO-66-NH_2 in water: stability, kinetic, isotherm and thermodynamic studies. J Colloids Interface Sci 461:79–87
Luu CL, Van Nguyen TT, Nguyen T, Hoang TC (2015) Synthesis, characterization and adsorption ability of UiO-66-NH_2. Adv Nat Sci Nanosci Nanotechnol 6:1–7
Maleki A, Hayati B, Naghizadeh M, Joo SW (2015) Adsorption of hexavalent chromium by metal organic frameworks from aqueous solution. J Ind Eng Chem 28:211–216
Malina J, Rađenović A (2014) Kinetic aspects of methylene blue adsorption on blast furnace sludge. Chem Biochem Eng 28:491–498
Mansoorian HJ, Mahvi AH, MostafaAlizadeh FKM (2013) Equilibrium and synthetic studies of methylene blue dye removal using ash of walnut shell. J Health Field 1:48–55
Masoumbeigi H, Rezaee A (2015) Removal of methylene blue (MB) dye from synthetic wastewater using UV/H_2O_2 advanced oxidation process. J Health Policy Sustain Health 2:160–166
Massoudinejad M, Ghaderpoori M, Shahsavani A, Amini MM (2016) Adsorption of fluoride over a metal organic framework Uio-66 functionalized with amine groups and optimization with response surface methodology. J Mol Liquid 221:279–286
Mohsenibandpei A, Ghaderpoori M, Hassani G, Bahrami H, Bahrami Z, Alinejad AA (2016) Water solution polishing of nitrate using potassium permanganate modified zeolite: parametric experiments. Kinet Equilib Anal 18:546–558
Peterson GW, DeCoste JB, Fatollahi-Fard F, Britt DK (2014) Engineering UiO-66-NH_2 for toxic gas removal. Ind Eng Chem Res 53:701–707
Rafatullah M, Sulaiman O, Hashim R, Ahmad A (2010) Adsorption of methylene blue on low-cost adsorbents: a review. J Hazard Mater 177:70–80
Reardon EJ, Wang Y (2000) A limestone reactor for fluoride removal from wastewaters. Environ Sci Technol 34:3247–3253
Saed UA, Nahrain MHA, Atshan AA (2014) Adsorption of methylene blue dye from aqueous solution using can papyrus. J Babylon Univ Eng Sci 22:218–229
Shahryari Z, Goharrizi AS, Azadi M (2010) Experimental study of methylene blue adsorption from aqueous solutions onto carbon nano tubes. Int J Water Resour Environ Eng 2:016–028
Shen L, Liang S, Wu W, Liang R, Wu L (2013a) Multifunctional NH_2-mediated zirconium metal-organic framework as an efficient visible-light-driven photocatalyst for selective oxidation of alcohols and reduction of aqueous Cr(VI)†. Dalton Trans 42:13649–13657
Shen L, Wu W, Liang R, Lin R, Wu L (2013) Highly dispersed palladium nanoparticles anchored on UiO-66(NH_2) metal-organic framework as a reusable and dual functional visible-light-driven photocatalyst. Royal Society Chemistry
Sohrabi MR, Ghavami M (2008) Photocatalytic degradation of direct red 23 dye using UV/TiO_2: effect of operational parameters. J Hazard Mater 153:1235–1239

Steel RGD, Torrie JH (1960) Principles and procedures of statistics (with special reference to the biological sciences). McGraw-Hill Book Company, New York, Toronto, London

Umoren SA, Etim UJ, Israel AU (2013) Adsorption of methylene blue from industrial effluent using poly (vinyl alcohol). J Mater Environ Sci 4:75–86

Vargas AMM, Cazetta AL, Kunita MH, Silva TL, Almeida VC (2011) Adsorption of methylene blue on activated carbon produced from flamboyant pods (Delonix regia): study of adsorption isotherms and kinetic models. Chem Eng J 168:722–730

Weng C-H, Pan Y-F (2007) Adsorption of a cationic dye (methylene blue) onto spent activated clay. J Hazard Mater 144:355–362

Xia G, Lu Y, Gao X, Gao C, Xu H (2014) Electro-Fenton degradation of methylene blue using polyacrylonitrile-based carbon fiber brush cathode. Clean Soil Air Water 42:1–8

Yola ML, Eren T, Atar N, Wang S (2014a) Adsorptive and photocatalytic removal of reactive dyes by silver nanoparticle-colemanite ore waste. Chem Eng J 242:333–340

Yola ML, Eren T, Atar N (2014b) A novel efficient photocatalyst based on TiO_2 nanoparticles involved boron enrichment waste for photocatalytic degradation of atrazine. Chem Eng J 250:288–294

Zhang N, Yang X, Yu X, Jia Y, Wang J, Kong L, Jin Z, Sun B, Luo T, Liu J (2014) Al-1,3,5-benzenetricarboxylic metal-organic frameworks: a promising adsorbent for defluoridation of water with pH insensitivity and low aluminum residual. Chem Eng J 252:220–229

Zhao X, Liu S, Tang Z, Niu H, Cai Y, Meng W, Wu F, Giesy JP (2015) Synthesis of magnetic metal-organic framework (MOF) for efficient removal of organic dyes from water. Sci Rep 5:1–10

Zhu BJ, Yu XY, Jia Y, Peng FM, Sun B, Zhang MY, Luo T, Liu JH, Huang XJ (2012) Iron and 1,3,5-benzenetricarboxylic metal-organic coordination polymers prepared by solvothermal method and their application in efficient As(V) removal from aqueous solutions. J Phys Chem C 116:8601–8607

Zvinowanda CM, Okonkwo JO, Sekhula MM, Agyei NM, Sadiku R (2009) Application of maize tassel for the removal of Pb, Se, Sr, U and V from borehole water contaminated with mine wastewater in the presence of alkaline metals. J Hazard Mater 164:884–891